Applied Surface Science 405 (2017) 178–182

Contents lists available at ScienceDirect

Applied Surface Science

journal homepage: www.elsevier.com/locate/apsusc

Gold particle formation via photoenhanced deposition on lithium niobate

A.M. Zaniewski*, V. Meeks, R.J. Nemanich

Arizona State University, Department of Physics, Tempe, AZ, United States

ARTICLE INFO

Article history:
Received 3 October 2016
Received in revised form 17 January 2017
Accepted 19 January 2017
Available online 24 January 2017

Keywords:
Nanoparticles
Gold
Lithium niobate

ABSTRACT

In this work, we report on a technique to reduce gold chloride into sub-micron particles and nanoparticles. We use photoelectron transfer from periodically polarized lithium niobate (PPLN) illuminated with above band gap light to drive the surface reactions required for the reduction and particle formation. The particle sizes and distributions on the PPLN surface are sensitive to the solution concentration, with inhibited nucleation and large particles (>150 nm) for both low (2E−8M to 9E−7M) and high (1E−5M to 1E−3M) concentrations of gold chloride. At midrange values of the concentration, nucleation is more frequent, resulting in smaller sized particles (<150 nm). We compare the deposition process to that for silver, which has been previously studied. We find that the reduction of gold chloride into nanoparticles is inhibited compared to silver ion reduction, due to the multi-step reaction required for gold particle formation. This also has consequences for the resulting deposition patterns: while silver deposits into nanowires along boundaries between areas with opposite signed polarizations, such patterning of the deposition is not observed for gold, for a wide range of concentrations studied (2E−8 to 1E−3M).

1. Introduction

Metallic nanostructures have a variety of unique optical [1], electronic [2], and catalytic properties [3]. Therefore, metal nanoparticles have been studied for a range of applications including: solar energy conversion [4,5]; information processing [6]; transparent conducting electrodes [7,8]; medicine [9]; and sensing [10].

Researchers have developed several techniques for controlling metal nanoparticle formation. For instance, thin films of metal evaporated onto lithographically defined masks provides the ability to pattern nanoparticles, but is a relatively expensive and time consuming approach [11]. On the other hand, if patterning is not a concern, simply heating thin metal films can result in their dewetting from the substrate surface to form islands [7,12], resulting in polydispersed particles.

Metal nanoparticles can also be formed in solution with in-situ reduction of metal salts into colloidal nanoparticles. Gold chloride reduction mediated by chemical reagents such as citrate is an example of this approach, which dates back to 1953 [13] and is still widely used and studied [14]. This technique requires relatively high temperatures, due to the weak reduction potential of citrate [15], and often involves the incorporation of stabilizing agents and surfactants [15]. Gold-citrate aggregates may form as a by-product of the citrate method [16]. Contemporary work on this reaction involves fine-tuning the pH [17], concentration [18], and order of reactions [19] in order to finely-control nanoparticle sizes. Such fine control over size is essential for tuning the optical properties of gold nanoparticles. By tuning the size of a gold nanoparticle, the wavelength of light which is resonant with the plasmonic excitation of the particle is correspondingly shifted [1].

In this work, we present an alternate technique for reducing gold chloride into nanoparticles: the photoexcitation of a polar insulating substrate acting as a driver for the reaction. In contrast with other in situ techniques, nanoparticle formation occurs at room temperature without additional reagents or stabilizing agents. In principle, this technique is similar to gold particle formation on surfaces such as silicate [20] or graphene [21]. However, in this case, the energy for the reaction comes from photoexcited electrons as opposed to oxidation of the surface.

The substrate we choose is lithium niobate, a ferroelectric semiconducting material. Ferroelectrics have the property of holding permanent polarizations and surface charge. By locally controlling the polarization of domains, the local reactivity of ferroelectrics can be controlled [22]. When illuminated with above-band gap light, internal electric fields drive photogenerated electrons to the

* Corresponding author.
E-mail addresses: azaniews@asu.edu, azaniewski@gmail.com (A.M. Zaniewski).

http://dx.doi.org/10.1016/j.apsusc.2017.01.201
0169-4332/

surface, preferentially to the positively-terminated domains and the boundaries between domains. These charges, in turn, enable surface reactions [23]. Thus, lithium niobate illuminated with above band gap light (>3.9 eV) has been used for the reduction of silver nitrate into silver nanoparticles [24]. Lithium niobate patterned to have alternating polarized domains, periodically polarized lithium niobate (PPLN), can be used to produce silver nanowires, as a result of the tendency of silver nanoparticles to preferentially form on the boundaries, consistent with the availability of electrons [25]. While lithium niobate has been the most ubiquitous substrate for these experiments, other ferroelectrics, such as lead zirconate titanate [26] and barium titanate [27] have also been studied for this technique.

Nanoparticles templated in such a manner may in principal be lifted from the ferroelectric and placed on a target substrate, and the ferroelectric template may be reused. Alternately, the nanoparticles can be left in place; this technique has been exploited for the growth of silver nanoparticles on PPLN for surface-enhanced Raman spectroscopy [28], controlled emission from Nd^+ [29] and enhanced emission from nanoscale lasers [30–32]. Lithium niobate also exhibits evanescent light-induced photovoltaic fields, which may be used as optical tweezers [33]; metallic nanoparticles could aid in this effort. Thus, beyond nanoparticle formation, this system holds promise for a range of nanophotonics applications.

While the deposition of silver on illuminated PPLN has been well established, there are fewer studies on the deposition of other materials with this technique. In this work, we explore the reduction of gold chloride into nanoparticles via illuminated PPLN. Park et al studied this process for a single gold chloride solution concentration, varying exposure times for the deposition [34]. This work contributes a concentration-dependent study and uses this concentration dependence to further understand nanoparticle growth on PPLN. We find that there is a substantial dependence on the concentration for the nucleation rate, size, and deposition pattern for gold nanoparticles. We also directly compare the gold nanoparticle deposition to that of silver. We find the silver and gold depositions to be quite dissimilar, even when accounting for optical absorption and molecule motility.

2. Materials and methods

The lithium niobate samples used have dimensions of 5 mm × 5 mm × 0.5 mm and come cut perpendicular to the polar axis, maximizing surface charge. The samples have a periodic polarization, and are obtained from Crystal Technologies. The polarizations have 180° domain walls. Prior to use, the PPLN substrates are cleaned via sonication for 10 min in acetone and methanol, and dried with nitrogen. The samples are then placed in a shallow petri dish, and a 25 μL drop of the gold (III) chloride or silver nitrate solution (Sigma–Aldrich) is added to the surface of the PPLN, forming a droplet of solution on the sample surface. To obtain the appropriate concentration, the solutions have been diluted with deionized water. The solutions are prepared and used at room temperature. No additional surfactants or catalysts are used. This small volume of solution is used to minimize absorption of the UV light by the solution itself.

A 100 W Hg lamp with a 254 nm bandpass filter serves as the UV light source. The intensity of the lamp is 850 μW/cm^2, and is measured prior to each experiment. The approximate spot size is 1 cm. The samples are kept under the UV lamp for 8 min. The samples are then rinsed in a water bath and dried with nitrogen.

Atomic force microscopy (Asylum MFP3D) with SiN probes that have a 10nm radius of curvature is used to measure the nanoparticles in place on the PPLN substrates. The scans are analyzed with ImageJ for statistical nanoparticle size and density analysis. This method was not sensitive to particles <10 nm in diameter.

3. Theory

The reaction required for gold chloride to form particles can proceed via several pathways. In particular, dissolving $HAuCl_4$ in water results in molecules of the form $AuCl_x$ where x may range from 2 to 4, with the percent of molecules of each species dependent upon the pH, with a lower x for more acidic solutions [35]. In our solutions the only source of acid is the $HAuCl_4$; thus the higher concentrations are more acidic. While a number of pathways for reduction are possible [36,37], here we describe one pathway starting from $AuCl_4$ to $AuCl_2$ [38].

$$AuCl_4^- + 2e^- \rightarrow AuCl_2^- + 2Cl^- \quad (1)$$

$$AuCl_2^- + e^- \rightarrow Au^0 + 2Cl^- \quad (2)$$

Since the solutions used contain a mixture of $AuCl_4$, $AuCl_3$ and $AuCl_2$, various reactions occur simultaneously. For those originating with $AuCl_4$ and $AuCl_3$, multiple steps are required to form Au^0.

For the silver nanoparticle formation, the reactions are more straightforward: silver nitrate in aqueous solution results in free Ag^+ ions. The formation of silver particles thus requires the addition of a single electron (from the PPLN surface) [25]:

$$Ag^+ + e^- \rightarrow Ag^0 \quad (3)$$

For both the silver and the gold reduction processes, there must be a corresponding oxidation reaction to maintain charge balance. The oxidizing reactions are facilitated by photogenerated holes from the surface of the lithium niobate and are expected to be:

$$2H_2O + 4h^+ \rightarrow O_2 + 4H^+ \quad (4)$$

The implications of these reactions for the deposition patterns of silver and gold nanoparticles are explored in the following section.

4. Results and discussion

Typical AFM results for select concentrations are shown in Fig. 1. The particle size and number density analysis is summarized in Table 1. For both high and low levels of gold chloride concentration, nanoparticle deposition is sparse, and particles tend to be large, >100 nm. However, for concentrations of 1E−7 to 2E−6, nanoparticles deposit with a high density and smaller average size (<100 nm). When discussing the size of the particles, we refer to the diameter of the base looking onto the surface of the samples.

While silver particles preferentially deposit on the boundary, resulting in nanowires, we do not observe this pattern for gold deposition, under the conditions studied.

To understand these deposition patterns, we consider the reaction dynamics of the system. We observe that since the particles are forming on the surface of the PPLN, the nucleation can be classified as a heterogeneous nucleation. Our observed results for gold particle nucleation fall into three cases. These three cases are illustrated schematically in Fig. 3 and summarized below:

- In the first case, the concentration of gold chloride is simply too low for the multi-step nucleation reaction. Nucleation is rare, and when it does occur, the nucleated particles grow to large sizes (≤ 2E−8M).
- In the second case, the increased flux of gold chloride ions on the surface allows for additional nucleation events to occur and particles are smaller. In addition, there are sufficient photoexcited

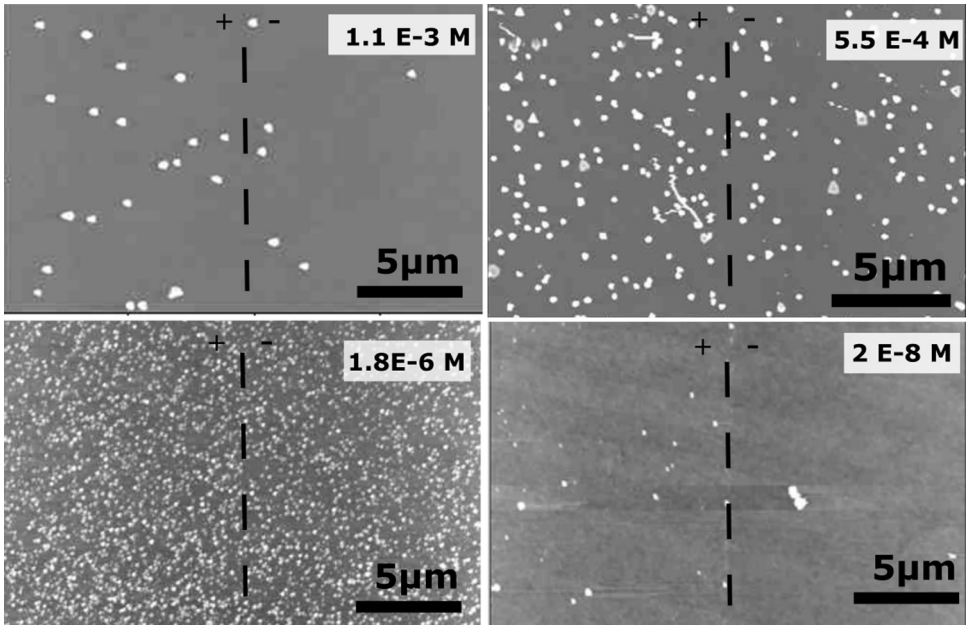

Fig. 1. Atomic force microscopy scans of gold particles on periodically poled lithium niobate (PPLN). The samples are made by adding an aqueous solution of gold chloride to the PPLN surface and illuminating the sample under ultraviolet light. Shown are samples corresponding to the following concentrations of gold chloride: 1.1 E−3M, 5.5 E−4M, 1.8 E−6M, and 2 E−8M.

Table 1
Results of depositions for various concentrations and metal species. The measurement technique was not sensitive to particles with diameters of <10 nm. Metal ion flux is the flux of silver or gold ions striking the PPLN surface calculated by the ion motility in water. Photon flux is determined based upon the optical absorption of the solution at the given concentration.

Concentration (M)	Metal	Metal ion flux Jb (1/s cm^2)	Photon flux Je (1/s cm^2)	Flux ratio (J_b/J_e)	Avg. diameter (nm)	Number per µm^2	Area covered (%)
1.00 E−3	Ag	3.63 E 21	9.33 E 14	3.90 E 06	78	10.8	5.13
1.10 E−3	Au	2.26 E 21	5.66 E 14	3.99 E 06	387	0.13	1.48
5.51 E−4	Au	1.13 E 21	7.87 E 14	1.44 E 06	274	0.92	5.41
2.76 E−4	Au	5.66 E 20	9.28 E 14	6.10 E 05	260	1.1	5.84
1.00 E−5	Au	2.05 E 19	1.09 E 15	1.88 E 04	180	1.23	3.14
1.00 E−6	Ag	3.63 E 18	1.09 E 15	3.32 E 03	104	2.2	1.87
1.80 E−6	Au	3.69 E 18	1.09 E 15	3.37 E 03	109	5.21	4.83
1.00 E−7	Au	2.05 E 17	1.09 E 15	1.87 E 02	69.9	10.1	3.87
9.10 E−7	Au	1.87 E 18	1.09 E 15	1.71 E 03	153	0.79	1.45
2.00 E−8	Au	4.10 E 16	1.09 E 15	3.75 E 01	170	0.17	0.38

electrons on the surface to enable these reductions (1E−7 to 2E−6M).

- In the third case, the high concentration of gold chloride (coupled with the charged surface of the PPLN) gives rise to a Stern layer. Excess chlorine ions form a barrier to auric salt molecules near the positive surface (where photogenerated electrons are most available), reducing the nucleation rate. The relative availability of photogenerated electrons is lower due to the increased optical absorption, and hence the reduction reaction is less probable (>1E−5M).

This concentration dependence on the particle size is similar to that for the citrate mediated gold chloride reduction theorized by Kumar et al. [39], which also results in large particles for high and low concentrations of gold chloride. However, in the Kumar model, large particles at high concentrations are explained by agglomeration; in our experiment, we do not anticipate that particles are mobile on the surface of the PPLN. Indeed, other studies of heterogeneous nucleation of metal nanoparticles find a concentration dependence on the nanoparticle size, without an agglomeration pathway for growth [40]. Instead, the large particles are a result of slow nucleation, a mechanism which has been observed in many other cases of nanoparticle formation [35,40–42].

We postulate that the difference between gold and silver deposition is due to the multi step nature of the nucleation reaction for gold: each gold salt ion interacts multiple times over a large average area, reducing the tendency of particles to form on the boundary between positive and negative domains.

To demonstrate that the distinction between silver and gold nanoparticle formation on PPLN is due to this multi-step chemistry and is not only a result of differing metal ion motility and optical absorption through the solution, we compare deposition for set metal ion:photon flux ratios. That is, we use optical absorption and ion motility calculations to have a similar number of gold or silver ions relative to photons striking the PPLN surface. The photon flux can be thought of as a proxy for the availability of excited electrons at the surface. Note that when we refer to metal ion flux we mean the number of metal ions (eg Ag+) impinging upon the PPLN surface per s cm^2, and are not referring to irradiation with an ion beam.

This ratio of metal ion:photon flux is calculated as below. Without any barriers such as a Stern layer, the flux of metal ions impinging upon the PPLN surface is approximated by [43]:

$$J_b = \sqrt{\frac{kT}{2\pi m}} C_o \tag{5}$$

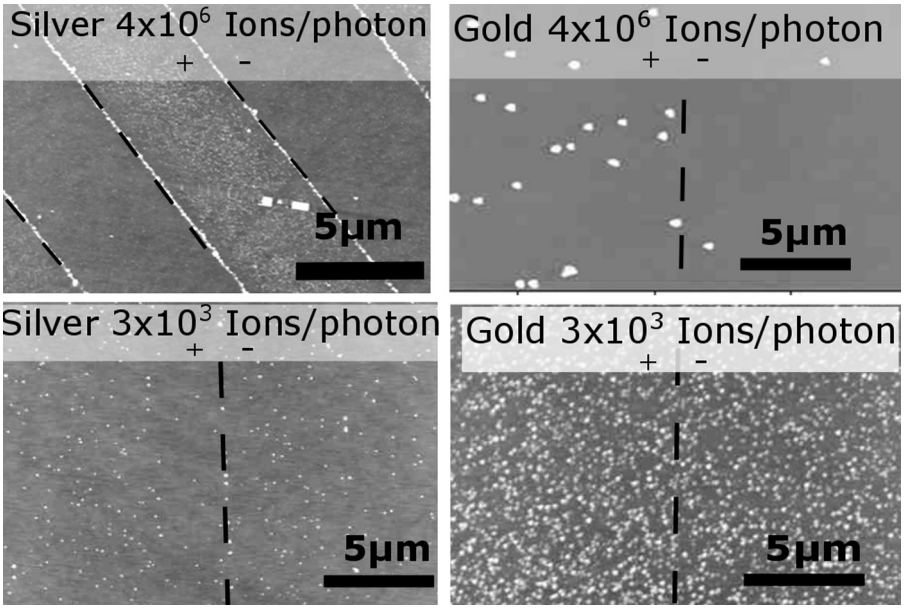

Fig. 2. Silver and gold particle deposition on PPLN for metal ion to photon ratios of 4E6 and 3E3. Despite having a similar ratio of available metal ions to excited electrons at the PPLN surface, the gold and silver deposition patterns are quite different, indicating the importance of the reduction mechanism for determining nanoparticle formation.

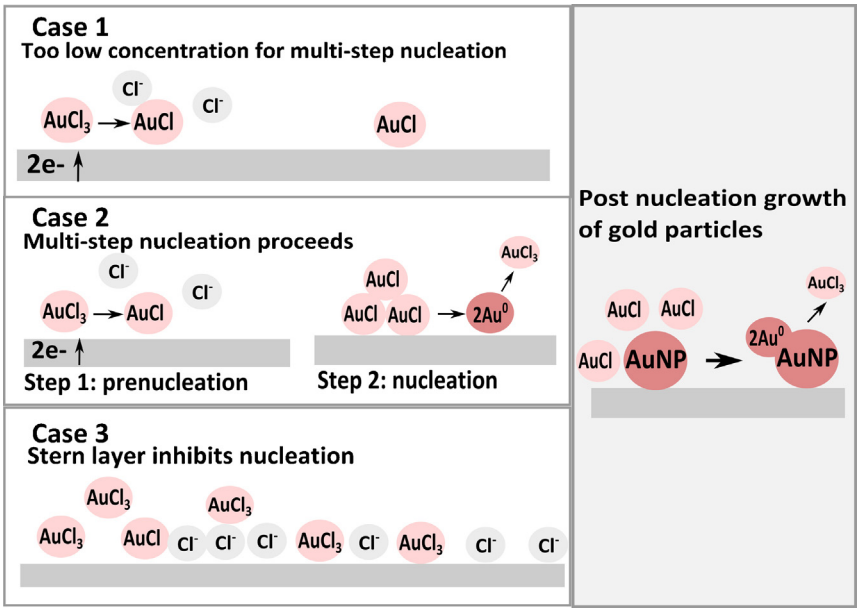

Fig. 3. Gold particle nucleation and growth model for one illustrative reduction reaction. Refer to Eqs. (1) and (2) for reduction reactions. Case 1: low concentrations (≤ 2E−8M) of gold chloride are insufficient for the multi-step nucleation reaction required. Nucleation is rare. Particles are sparse and large. Case 2: mid concentrations (1E−7 to 2E−6M) of gold chloride result in multiple nucleation sites, indicative of multi-step reactions proceeding uninhibited or with sufficient acidity to generate $AuCl_2$. Nucleation is frequent, and particles are small. Case 3: high concentrations (>1E−5M) result in inhibited nucleation reactions, likely as a result of a Stern layer on the surface. Nucleation events are rare, and particles are large.

where k is the Boltzmann constant, T is temperature in Kelvin, m is the mass of the particle, C_o is the concentration of the particles in solution near the surface and the units of flux are given in $cm^{-2}\ s^{-1}$.

Similarly, the photon flux is calculated by Planck's law and the Beer–Lambert law:

$$J_e = \frac{I\lambda}{hc} e^{-\sigma l C_o} \tag{6}$$

where I is the intensity of the UV source measured in W/cm^2, λ is the wavelength (254 nm), h is Planck's constant, c is the speed of light, l is the path length, and σ is the attenuation cross section determined by UV–Vis spectroscopy.

Fig. 2 shows two cases where silver and gold concentrations should have identical flux ratios (metal ion:photon ratio is 3E3 and 4E6, respectively). Clearly, the particle deposition pattern is quite distinct for the different metal species. This indicates that the molecule size and optical absorption of the solution alone are insufficient predictors of nanoparticle deposition, and factors such as the probability of each reaction step and existence of the Stern layer must be taken into account.

At a metal ion:photon flux ratio of 4E6, silver deposition results in nanowire formation, shown in Fig. 2. This is in agreement with prior work [25] on silver nanoparticle deposition. The tendency of silver ions to deposit as nanowires disappears for lower flux ratios

(<1E4); instead, particles form over the domain surfaces. At the flux ratio of 3E3, silver deposition is quite sparse, as shown in Fig. 2, but gold deposition is at its peak density. However, for the parameter space studied in this work, continuous gold nanowires do not form, regardless of the gold chloride concentration.

5. Conclusions

In conclusion, we find that UV illuminated PPLN can be used as a reducing surface for gold chloride, resulting in gold particles, and the size of the particles is highly sensitive to the concentration of the gold chloride. No surfactants or reagents are used: deposition occurs as a result of interaction with the photo-excited PPLN surface. The mechanism for gold reduction is explored, and the chemistry of this reaction plays a critical role in the resulting deposition patterns. Gold nanoparticles on lithium niobate could find a variety of photonic applications such as plasmonically enhanced lithium niobate lasers, or surface-enhanced Raman spectroscopy. The deposition of gold nanoparticles differs from silver in that gold does not readily form nanowires; further exploration will be required to determine if gold nanowires can be achieved with this technique.

Acknowledgements

This work is supported through the National Science Foundation under Grant # DMR-1206935. We gratefully acknowledge the use of facilities with the LeRoy Eyring Center for Solid State Science at Arizona State University. We thank Yang Sun for UV–Vis data, and Brandon Palafox for material preparation. VM acknowledges support from the Arizona NASA Space Grant Internship program.

References

[1] K.L. Kelly, E. Coronado, L.L. Zhao, G.C. Schatz, The optical properties of metal nanoparticles: the influence of size, shape, and dielectric environment, J. Phys. Chem. B 107 (3) (2003) 668–677.
[2] M.-C. Daniel, D. Astruc, Gold nanoparticles: assembly, supramolecular chemistry, quantum-size-related properties, and applications toward biology, catalysis, and nanotechnology, Chem. Rev. 104 (1) (2004) 293–346.
[3] J. Zeng, Q. Zhang, J. Chen, Y. Xia, A comparison study of the catalytic properties of Au-based nanocages, nanoboxes, and nanoparticles, Nano Lett. 10 (1) (2009) 30–35.
[4] S. Linic, P. Christopher, D.B. Ingram, Plasmonic–metal nanostructures for efficient conversion of solar to chemical energy, Nat. Mater. 10 (12) (2011) 911–921.
[5] K. Catchpole, A. Polman, Plasmonic solar cells, Opt. Express 16 (26) (2008) 21793–21800.
[6] N. Engheta, Circuits with light at nanoscales: optical nanocircuits inspired by metamaterials, Science 317 (5845) (2007) 1698–1702.
[7] A.M. Zaniewski, M. Schriver, J.G. Lee, M. Crommie, A. Zettl, Electronic and optical properties of metal-nanoparticle filled graphene sandwiches, Appl. Phys. Lett. 102 (2) (2013) 023108.
[8] D.S. Hecht, L. Hu, G. Irvin, Emerging transparent electrodes based on thin films of carbon nanotubes, graphene, and metallic nanostructures, Adv. Mater. 23 (13) (2011) 1482–1513.
[9] E.C. Dreaden, A.M. Alkilany, X. Huang, C.J. Murphy, M.A. El-Sayed, The golden age: gold nanoparticles for biomedicine, Chem. Soc. Rev. 41 (7) (2012) 2740–2779.
[10] K.-S. Lee, M.A. El-Sayed, Gold and silver nanoparticles in sensing and imaging: sensitivity of plasmon response to size, shape, and metal composition, J. Phys. Chem. B 110 (39) (2006) 19220–19225.
[11] M. Feldman, Nanolithography: The Art of Fabricating Nanoelectronic and Nanophotonic Devices and Systems, Woodhead Publishing Series in Electronic and Optical Materials, Elsevier Science, 2014.
[12] J. Huang, F. Kim, A.R. Tao, S. Connor, P. Yang, Spontaneous formation of nanoparticle stripe patterns through dewetting, Nat. Mater. 4 (12) (2005) 896–900.
[13] J. Turkevich, P.C. Stevenson, J. Hillier, The formation of colloidal gold, J. Phys. Chem. 57 (7) (1953) 670–673.
[14] X. Ji, X. Song, J. Li, Y. Bai, W. Yang, X. Peng, Size control of gold nanocrystals in citrate reduction: the third role of citrate, J. Am. Chem. Soc. 129 (45) (2007) 13939–13948.
[15] P. Zhao, N. Li, D. Astruc, State of the art in gold nanoparticle synthesis, Coordinat. Chem. Rev. 257 (34) (2013) 638–665, http://dx.doi.org/10.1016/j.ccr.2012.09.002 http://www.sciencedirect.com/science/article/pii/S0010854512002305.
[16] M. Doyen, K. Bartik, G. Bruylants, UV–Vis and NMR study of the formation of gold nanoparticles by citrate reduction: observation of gold-citrate aggregates, J. Colloid Interface Sci. 399 (2013) 1–5.
[17] H. Tyagi, A. Kushwaha, A. Kumar, M. Aslam, A facile pH controlled citrate-based reduction method for gold nanoparticle synthesis at room temperature, Nanoscale Res. Lett. 11 (1) (2016) 362.
[18] K. Zabetakis, W.E. Ghann, S. Kumar, M.-C. Daniel, Effect of high gold salt concentrations on the size and polydispersity of gold nanoparticles prepared by an extended Turkevich–Frens method, Gold Bull. 45 (4) (2012) 203–211.
[19] I. Ojea-Jimenez, N.G. Bastús, V. Puntes, Influence of the sequence of the reagents addition in the citrate-mediated synthesis of gold nanoparticles, J. Phys. Chem. C 115 (32) (2011) 15752–15757.
[20] S. Mohammadnejad, J.L. Provis, J.S. van Deventer, Reduction of gold (III) chloride to gold (0) on silicate surfaces, J. Colloid Interface Sci. 389 (1) (2013) 252–259.
[21] A.M. Zaniewski, C.J. Trimble, R.J. Nemanich, Modifying the chemistry of graphene with substrate selection: a study of gold nanoparticle formation, Appl. Phys. Lett. 106 (12) (2015) 123104.
[22] S.V. Kalinin, D.A. Bonnell, T. Alvarez, X. Lei, Z. Hu, J. Ferris, Q. Zhang, S. Dunn, Atomic polarization and local reactivity on ferroelectric surfaces: a new route toward complex nanostructures, Nano Lett. 2 (6) (2002) 589–593.
[23] D. Tiwari, S. Dunn, Photochemistry on a polarisable semi-conductor: what do we understand today? J. Mater. Sci. 44 (19) (2009) 5063–5079.
[24] S. Dunn, S. Sharp, S. Burgess, The photochemical growth of silver nanoparticles on semiconductor surfaces initial nucleation stage, Nanotechnology 20 (11) (2009) 115604.
[25] Y. Sun, B.S. Eller, R.J. Nemanich, Photo-induced Ag deposition on periodically poled lithium niobate: concentration and intensity dependence, J. Appl. Phys. 110 (8) (2011) 084303.
[26] S. Dunn, P.M. Jones, D.E. Gallardo, Photochemical growth of silver nanoparticles on C^- and C^+ domains on lead zirconate titanate thin films, J. Am. Chem. Soc. 129 (28) (2007) 8724–8728.
[27] J.L. Giocondi, G.S. Rohrer, Spatially selective photochemical reduction of silver on the surface of ferroelectric barium titanate, Chem. Mater. 13 (2) (2001) 241–242.
[28] S. Damm, N.C. Carville, B.J. Rodriguez, M. Manzo, K. Gallo, J.H. Rice, Plasmon enhanced Raman from Ag nanopatterns made using periodically poled lithium niobate and periodically proton exchanged template methods, J. Phys. Chem. C 116 (50) (2012) 26543–26550.
[29] E. Yraola, L. Sánchez-García, C. Tserkezis, P. Molina, M. Ramírez, J. Aizpurua, L. Baus, Polarization-selective enhancement of Nd^3+ photoluminescence assisted by linear chains of silver nanoparticles, J. Lumin. 169 (2016) 569–573.
[30] P. Molina, E. Yraola, M.O. Ramírez, J.L. Plaza, C. de las Heras, L.E. Bausaí, Selective plasmon enhancement of the 1.08 μm Nd^3+ laser stark transition by tailoring Ag nanoparticles chains on a PPLN Y-cut, Nano Lett. 3 (10) (2013) 4931–4936.
[31] E. Yraola, P. Molina, J.L. Plaza, M.O. Ramírez, L.E. Baus, Spontaneous emission and nonlinear response enhancement by silver nanoparticles in a Nd^3+-doped periodically poled $LiNbO_3$ laser crystal, Adv. Mater. 25 (6) (2013) 910–915.
[32] Y. Ge, J. Cao, Z. Shen, Y. Zheng, X. Chen, W. Wan, Terahertz wave generation by plasmonic-enhanced difference-frequency generation, JOSA B 31 (7) (2014) 1533–1538.
[33] J. Villarroel, H. Burgos, Á. García-Caba nes, M. Carrascosa, A. Blázquez-Castro, F. Agulló-López, Photovoltaic versus optical tweezers, Opt. Express 19 (24) (2011) 24320–24330.
[34] Y.-S. Park, J.-H. Kim, W. Yang, Comparison study of metal nanoparticles grown on polarity-patterned ferroelectrics by scanning probe microscopy, Surf. Interface Anal. 44 (6) (2012) 759–762.
[35] S. Wang, K. Qian, X. Bi, W. Huang, Influence of speciation of aqueous $HAuCl_4$ on the synthesis, structure, and property of au colloids, J. Phys. Chem. C 113 (16) (2009) 6505–6510, http://dx.doi.org/10.1021/jp811296m.
[36] J. Yannopoulos, The Extractive Metallurgy of Gold, Van Nostrand Reinhold, 1991.
[37] F.A. Cotton, G. Wilkinson, C.A. Murillo, M. Bochmann, Adv. Inorgan. Chem. 6 (1999).
[38] J.K. Young, N.A. Lewinski, R.J. Langsner, L.C. Kennedy, A. Satyanarayan, V. Nammalvar, A.Y. Lin, R.A. Drezek, Size-controlled synthesis of monodispersed gold nanoparticles via carbon monoxide gas reduction, Nanoscale Res. Lett. 6 (1) (2011) 1.
[39] S. Kumar, K. Gandhi, R. Kumar, Modeling of formation of gold nanoparticles by citrate method, Ind. Eng. Chem. Res. 46 (10) (2007) 3128–3136.
[40] Y. Wang, X. Xu, Z. Tian, Y. Zong, H. Cheng, C. Lin, Selective heterogeneous nucleation and growth of size-controlled metal nanoparticles on carbon nanotubes in solution, Chem.-A Eur. J. 12 (9) (2006) 2542–2549.
[41] G. Cao, Y. Wang, Nanostructures and Nanomaterials: Synthesis, Properties, and Applications, in: World Scientific Series in Nanoscience and Nanotechnology, World Scientific, 2011.
[42] T. Teranishi, M. Hosoe, T. Tanaka, M. Miyake, Size control of monodispersed pt nanoparticles and their 2d organization by electrophoretic deposition, J. Phys. Chem. B 103 (19) (1999) 3818–3827, http://dx.doi.org/10.1021/jp983478m.
[43] S. Giuffrida, G.G. Condorelli, L.L. Costanzo, I.L. Fragalá, G. Ventimiglia, G. Vecchio, Photochemical mechanism of the formation of nanometer-sized copper by UV irradiation of ethanol bis (2, 4-pentandionato) copper (II) solutions, Chem. Mater. 16 (7) (2004) 1260–1266.